JQS   Journal of Quaternary Science   QRA

Climate and atmospheric circulation during the Early and Mid-Holocene inferred from lake-carbonate oxygen-isotope records from western Ireland

JONATHAN A. HOLMES,[1]* [iD] JULIA TINDALL,[2] MATTHEW JONES,[3] MAX HOLLOWAY,[4] NEIL ROBERTS[5] [iD] and INGO FEESER[6]

[1]Environmental Change Research Centre, Department of Geography, University College London, London, UK
[2]School of Earth and Environment, University of Leeds, Leeds, UK
[3]School of Geography, University of Nottingham, Nottingham, UK
[4]SAMS, Scottish Marine Institute, Oban, Argyll, UK
[5]School of Geography, Earth and Environmental Sciences, University of Plymouth, Plymouth, UK
[6]Institute of Pre- and Protohistoric Archaeology, Kiel University, Kiel, Germany

ABSTRACT: The Early to Mid-Holocene experienced marked climate change over the northern hemisphere mid-latitudes in response to changing insolation and declining ice volume. Oxygen isotopes from lake sediments provide a valuable climate proxy, encoding information regarding temperature, hydroclimate and moisture source. We present oxygen-isotope records from two lakes in western Ireland that are strongly influenced by the North Atlantic. Excellent replication between the records suggests they reflect regional, not local, influences. Carbonate oxygen-isotope values peaked at the start of the Holocene, between 11.2 and 11.1 cal ka BP, and then decreased markedly until 6 cal ka BP at both sites. Palaeoecological evidence supports only modest change in temperature or hydroclimate during this interval and we therefore explain the decrease primarily by a reduction in the oxygen-isotope composition of precipitation ($\delta^{18}O_{ppt}$). We show a similar decrease in $\delta^{18}O$ values in a forward model of carbonate isotopes between 12–11 and 6–5 cal ka BP. However, the inferred reduction in $\delta^{18}O_{ppt}$ between the Early and Mid-Holocene in the model is mainly linked to a decrease in the $\delta^{18}O$ of the ocean source water from ice sheet melting whereas the lake carbonate isotope records are more consistent with changes in the transport pathway of moisture associated with atmospheric circulation change as the dominant cause.
© 2023 The Authors. *Journal of Quaternary Science* Published by John Wiley & Sons Ltd.

KEYWORDS: Holocene; lake sediments; oxygen isotopes; western Ireland

Introduction

The Holocene (11.7 cal ka BP to present) is of considerable interest as the most recent interglacial and a time during which major changes in the physical and biological landscape have occurred, along with significant developments in human cultural evolution. Although the amplitude of pre-industrial climatic variations during the Holocene was muted at mid-latitudes compared with those of the last glacial stage, it has still been characterized by significant climatic trends (Carlson et al., 2008) as well as abrupt events (Mayewski et al., 2004). The study of such trends and events provides an important baseline for evaluating natural versus anthropogenically induced climatic change. Compilations of marine and terrestrial climate proxy data reveal contrasting patterns in the detail of Holocene temperature change (Marcott et al., 2013; Marsicek et al., 2018; Kaufman et al., 2020; Bova et al., 2021; Hertzberg, 2021; Liu et al., 2014; Erb et al., 2022) although a sharp rise in temperature for the first few thousand years of the Holocene is evident in most northern hemisphere compilations in spite of the summer insolation maximum at this time and has been attributed to the influence of the remnant Laurentide ice sheet (Renssen et al., 2009). Evidence also exists for reorganization of atmospheric circulation during the Holocene, especially in the North Atlantic sector with some studies suggesting a change from a more meridional pattern of atmospheric circulation (Baker et al., 2017) and shifts in the North Atlantic Oscillation (NAO) (Wassenburg et al., 2016). These have been attributed to the demise of the Laurentide ice sheet and associated shifts in the jet stream, as well as shorter term changes linked to ocean–atmosphere interactions (Smith et al., 2016; Goslin et al., 2018). However, some evidence suggests contrasting patterns of atmospheric circulation, with a more zonal pattern for the Early to Mid-Holocene and an intensification of zonal flow (e.g. Hammarlund et al., 2002; Seppä et al., 2005). In short, although there are good theoretical reasons to expect that atmospheric circulation has changed during the Holocene, along with empirical evidence demonstrating such change, the precise nature and causes of these changes remain unclear.

In this paper, we describe Early to Mid-Holocene oxygen-isotope records from two neighbouring lakes in western Ireland, along with palaeoecological evidence from one of them, and discuss their implications for changes in atmospheric circulation during the first half of the Holocene, when changes in forcing and boundary conditions were marked (Törnqvist & Hijma, 2012; Marcott et al., 2013). We also compare the records with results from the isotope-enabled general circulation model iHadCM3, in order to assess

*Correspondence Jonathan A. Holmes, as above.
E-mail: j.holmes@ucl.ac.uk

whether this model is able to produce realistic simulations of changes in oxygen isotopes during the Early to Mid-Holocene.

Oxygen isotopes are excellent tracers of past climate (Konecky et al., 2020), particularly changes in hydroclimate and atmospheric circulation (Hammarlund et al., 2002; Baker et al., 2017). The oxygen-isotope composition of lacustrine carbonate encodes information from multiple controls, the relative importance of which will depend on the climatic, hydrological and topographical setting of the lake (Leng and Marshall, 2004). So, although lake-sediment oxygen-isotope records are valuable proxies for past climate, they require careful evaluation to deconvolve what are often complex signals. Fundamentally, the oxygen-isotope composition of lacustrine carbonate is determined by the temperature and isotopic composition of the lake water from which the carbonate precipitates, along with disequilibrium effects that are often seen in biogenic carbonate or when precipitation rates are high (Leng and Marshall, 2004). The oxygen-isotope composition of lake water is determined by the composition of inputs (direct precipitation, runoff and groundwater) together with heavy-isotope enrichment by evaporation, which is a characteristic of lakes with long residence times (Leng and Marshall, 2004). The composition of groundwater and runoff are closely related to the isotopic composition of rainwater, which is in turn determined by a range of factors including condensation temperate, rainfall amount and source, transport pathway, and rainout history of the air mass (Dansgaard, 1964). Deconvolving carbonate oxygen-isotope records, and especially distinguishing regional climatic controls from basin-specific factors, can be achieved in several ways, including the use of oxygen-isotope records from other minerals or biomolecules such as chitin (Verbruggen et al., 2010b), aquatic cellulose (Street-Perrott et al., 2018) or diatom silica (Leng et al., 2001), determining the role of water isotope composition by employing independent temperature proxies such as pollen (Hammarlund et al., 2002) or chironomids (Marshall et al., 2007), or using models (Jones and Dee, 2018). Studies into the modern oxygen-isotope systematics of an extant lake also contribute to interpretation of lake-sediment records (Jones et al., 2016a). Western Ireland is ideally located to record changes in atmospheric circulation; its position makes it especially sensitive to conditions over the adjacent North Atlantic Ocean (Diefendorf and Patterson, 2005), which are important mediators of Holocene climate across Europe, in particular. The study of paired lakes within a small geographical area, as in the present investigation, allows regional climate trends to be distinguished from basin-specific variations that may not be closely related to climate.

Site description

Regional information

This study is based on sediments from Lough Gealáin and Lough Avolla, two neigbouring lakes in the Burren, an area of glaciokarstified Carboniferous limestone in Co. Clare, western Ireland. The Burren consists of an upland plateau as well as adjacent lowlands, on which the two study sites are located (Fig. 1).

Western Ireland experiences an oceanic climate (mean annual temperature = 10.3 °C; mean annual precipitation = 1189 mm) with mild wet winters (mean January temperature = 5.8 °C; mean winter precipitation = 341 mm) and cool wet summers (mean July temperature = 15.6 °C; mean summer precipitation = 252 mm) (National University of Ireland, Galway, Galway City: Gaffney, 2006). A long (1957 to present) GNIP (Global Network of Isotopes in Precipitation: IAEA/WMO, 2022) record of the isotopic composition of monthly precipitation ($\delta^{18}O_{ppt}$ and δ^2H_{ppt}) from Valentia, 150 km southwest by south of the two Burren lakes (Fig. 1), has a mean annual weighted $\delta^{18}O_{ppt}$ of -5.52 ± 0.56‰ VSMOW, with winter values (December to February, weighted $\delta^{18}O_{ppt}$ of -5.96‰ VSMOW) more ^{18}O depleted than summer values (June to August, weighted $\delta^{18}O_{ppt}$ of -4.28‰ VSMOW). The oxygen-isotope composition of groundwater ($\delta^{18}O_{gw}$) on an
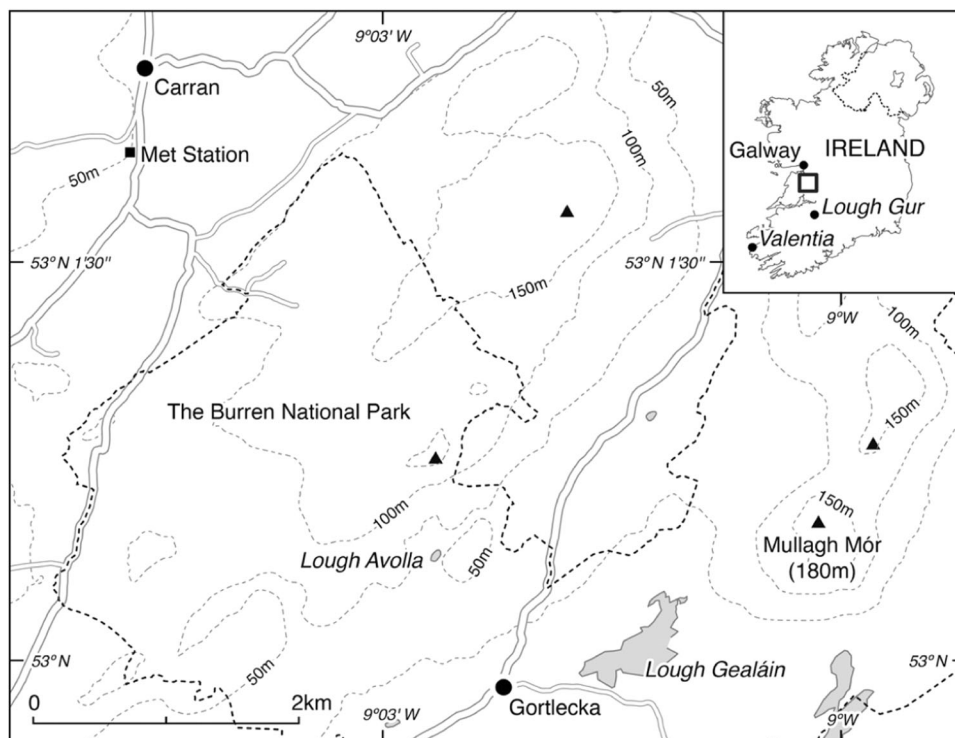

Figure 1. Location of the study sites and other localities mentioned in the text.

area of karstified limestone around 15 km north of the study lakes ranged from −6.7 to −6.1‰ VSMOW, suggesting preferential recharge by winter rainfall (Einsiedl, 2012). Ground water tracing experiments (Drew, 1988) indicate that groundwater from the eastern flank of the Burren uplands drains into the lakes of the adjacent lowlands, suggesting that Lough Avolla and Lough Gealáin are part of a single hydrogeological system. A survey of surface waters across Ireland, including the Burren, shows that the isotopic composition of some lakes has been modified by evaporation (Diefendorf and Patterson, 2005).

Lough Gealáin

Lough Gealáin (52°59.95′N; 9°1.30′W) lies 30 m a.s.l. within a depression in the lowlands immediately beyond the edge of the Burren Plateau. The basin comprises a permanent lake, with an area of about 12 ha and maximum depth of 13 m, and a non-permanent 'turlough' (a seasonal waterbody), which lies to the west of the main lake and usually dries out in summer. The seasonal variation in water level of the main lake is ~3 m, related to changes in height of the water table. Lough Gealáin is surrounded by bare karstified limestone, with patches of hazel scrub and a small area of tall-canopy woodland.

Lough Avolla

Lough Avolla (53°0.34′N; 9°2.67′W) lies 90 m a.s.l. within a deep, sheltered depression 1.7 km northwest of Lough Gealáin (Marshall, 2002). Lough Avolla has an area of 0.32 ha and is ~6 m deep although lake level oscillates seasonally, with a 20–50-m-wide wetland fringe that is flooded during high-stands. The basin supports pasture and scrub on glacial till adjacent to the lake and thinly vegetated bedrock on the surrounding plateau.

Materials and methods
Modern water samples

To augment the GNIP data, monthly measurements of $\delta^{18}O_{ppt}$ and δ^2H_{ppt} were made from rainfall collected between June 2004 and December 2005 at Carran, which lies at 130 m a.s.l. and several kilometres to the northwest of the study lakes (Fig. 1), following IAEA sampling protocols (IAEA/GNIP, 2014). Lake water samples from Lough Gealáin were also analysed for oxygen and hydrogen isotopes over the same period: a few spot samples were taken at other times. Only occasional samples of water were collected from Lough Avolla and its inflowing springs, owing to restrictions on access to this site. Oxygen-isotope ratios were determined on 2.5 mL of water using standard CO_2 equilibration (Epstein and Mayeda, 1953; Horita and Kendall, 2004) at 25 °C for 48 h in a water bath. Following equilibration, CO_2 was removed cryogenically and analysed using a VG SIRA 10 mass spectrometer: results are expressed in standard delta notation relative to VSMOW with uncertainty of ±0.04‰ (1σ). Hydrogen-isotope ratios were measured on hydrogen gas extracted from 2 mL of water samples by high-temperature Zn reduction (Coleman et al., 1982; Horita & Kendall, 2004) using a VG SIRA 12 mass spectrometer. Isotope ratios are reported in standard delta notation relative to VSMOW, with analytical precision of ±0.6‰ (1σ).

Lake sediments

Core LA2B was recovered from the southwestern margin of Lough Avolla using a Livingstone piston corer. Core MLM8 was recovered from the marl shelf from the southern edge of the permanent part of Lough Gealáin using a Usinger piston corer. The chronology for both cores was provided by accelerator mass spectrometry (AMS) radiocarbon dates derived from terrestrial plant macrofossils, with some additional alignment based on lithostratigraphical markers. Age–depth modelling was performed using CLAM version 2.3.2 (Blaauw, 2010), with calibration of radiocarbon ages undertaken using IntCal13 (Reimer et al., 2013).

Bulk sediment samples were treated with Clorox to remove organic material (Mannella et al., 2020), and then sieved through a 125-μm mesh to remove shell material and isolate the fine endogenic fraction, which was then analysed using a ThermoFinnegan Delta Plus XP mass spectrometer connected to a GasBench. Results are reported in standard delta notation relative to VPDB with analytical precision of ±0.08‰ (1σ). Microscopic investigations confirmed the absence of detrital carbonate grains from the marl sediments and we therefore assume that the isotopic composition of carbonates from cores MLM8 and LA2B is reflective of conditions in the respective lakes at the time of carbonate precipitation.

Pollen data from MLM8 were used to constrain Early to Mid-Holocene temperatures and precipitation patterns for the Burren to support interpretation of the oxygen-isotope records. Samples for pollen analysis were prepared using standard methods including KOH, HCl, acetolyses and HF treatment (cf. Moore et al., 1991). After an initial sieving, the residues (>100 μm) were examined under the stereomicroscope for macrofossil remains and carbonate concretion morphotypes (Magny 2007). Further details are provided in Feeser (2009). Only selected data relevant to the interpretation of the oxygen-isotope records are presented and discussed here. Sediments from MLM8 and LA2B were analysed for organic carbon content and carbonate content using loss-on-ignition at 550 and 950 °C, respectively, following Heiri et al. (2001).

To further help interpret the changes in oxygen isotope in the lake sediments, we utilized the isotope-enabled version of the HadCM3 general circulation model (iHadCM3) (Gordon et al., 2000, Pope et al., 2000, Tindall et al., 2009). Simulations were run at 1000-year intervals from 11 to 5 cal ka BP and the model was forced with orbital parameters, greenhouse gases and ice sheets based on Singarayer and Valdes (2010). A correction ranging from 0.39‰ at 11 cal ka BP to 0.02‰ at 5 cal ka BP (Lambeck et al., 2014) was applied to all modelled $\delta^{18}O_{ppt}$ values to account for the changes in ice volume. To facilitate comparison of the lake-sediment records with the results of modelling experiments, modelled values of temperature, precipitation and $\delta^{18}O_{ppt}$ taken from iHadCM3 for the grid square with coordinates 52.5°N, 11.25°W were combined to produce a synthetic record of $\delta^{18}O_{CaCO3}$ for each 1000-year time-slice from 11 to 5 cal ka BP. Monthly values of the amount and $\delta^{18}O$ of precipitation were used to determine the weighted annual precipitation values, which were in turn used to approximate the $\delta^{18}O$ of lake water ($\delta^{18}O_{lake}$), under the assumption that evaporation has not significantly modified the isotopic composition of the lakes. The $\delta^{18}O_{lake}$ values were then combined with summer temperature to approximate the conditions under which carbonate precipitation took place, and the $\delta^{18}O_{CaCO3}$ was calculated using the equation of Kim and O'Neil (1997). Although the chosen grid square sits over the Atlantic Ocean, we consider it the most appropriate to use. This is because $\delta^{18}O_{ppt}$ values over land masses in iHadCM3 are impacted by rainout effects, especially so for Ireland in

summer, and these rainout effects are unlikely to impact the lake sites considered here given their proximity to the coast.

Results

Modern waters

The weighted mean $\delta^{18}O_{ppt}$ at Carran over the sampling period was −6.0‰, which is consistent with the mean value for Valentia (−5.5‰) (Fig. 2a and B), given the inland location and higher elevation of the former. Lake waters from Lough Gealáin had a more positive mean $\delta^{18}O_{lake}$ value of −5.1 ± 0.6‰ although this falls on a local meteoric water line (LMWL) defined by Carran precipitation (Fig. 2b). Monthly values of $\delta^{18}O_{lake}$ from Lough Gealáin follow local precipitation values (Fig. 2c), albeit damped, which is typical of open lakes in the British Isles (Tyler et al., 2007, Jones et al., 2016b). The lake shows no significant isotopic response to the seasonal variation in water level, suggesting that this variation is not the result of evaporation but rather to seasonal changes in the height of the water table (Fig. 2c). There is only slight isotopic depth stratification of Lough Gealáin (Fig. 2d), probably because of wind mixing at this exposed site. The $\delta^{18}O_{lake}$ values for Lough Avolla are too few to be able to draw firm conclusions although the mean $\delta^{18}O_{lake}$ value of −6.4‰ places the values close to the LMWL. The mean value is ~1‰ more negative than that for Lough Gealáin, but strongly influenced by two low values relating to spot samples from the lake (Fig. 2b).

Lake-sediment chronology

Core MLM8 from Lough Gealáin consists of 6.02 m of marl overlain by silty clay, marl and then peat (Fig. 3): a thin layer of marl overlying the peat is present in parallel core MLM7 but absent from MLM8. The Holocene section of core LA2B from Lough Avolla is 7.38 m long and composed of marl and organic marl and finally peat (Fig. 3). An age model for MLM8 in cal years BP was constructed using a combination of radiocarbon dates and a lithological marker for the start of the Holocene, for which a radiocarbon age of 10 000 a BP was adopted (Gibbard et al., 2020). Nine radiocarbon dates were obtained from core MLM8 of which seven were used in the age–depth model for the core (Table 1) (Fig. 4). The two excluded radiocarbon dates are from the peat above 133 cm, which has a contrasting sedimentation rate to the underlying marl. The sharp lithological change from highly minerogenic sediment to marl at 595 cm in MLM8 is assumed to mark the start of the Holcene. The pollen spectra (Feeser, 2009) and the sharp rise in $\delta^{18}O_{CaCO3}$ at this level (Fig. 3b) support this interpretation. A similar lithological transition linked to palynological evidence marking the onset of the Holocene has been noted from the nearby Aran Islands (O'Connell and Molloy, 2005). The radiocarbon dates were calibrated and an age–depth curve constructed using classical age–depth modelling with CLAM (Blaauw, 2010) in order to provide age estimates, in calendar years BP, for each level in the core. An age model for LA2B was constructed in a similar way. The transition from minerogenic sediment to marl, which is used to mark the start of the Holocene, occurs at 737 cm depth in LA2B. Nine radiocarbon dates were
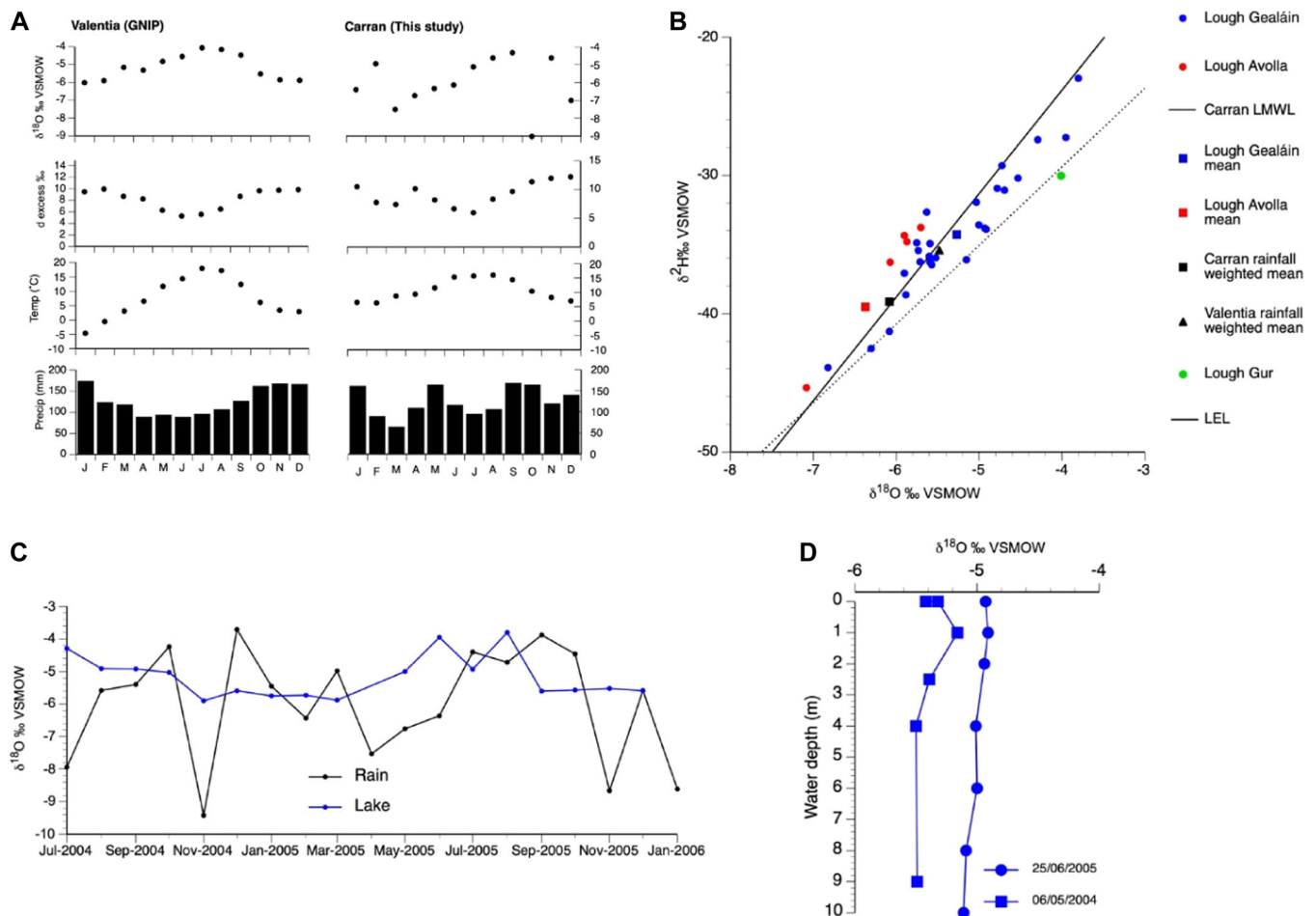

Figure 2. (A) $\delta^{18}O$ of monthly rainfall from Valentia (from GNIP) 1957–2015, and Carran (this study). (B) $\delta^{18}O$ and δ^2H of rainfall and lake water. Carran LMWL = local meteoric water line for Carran rainfall. LEL = local evaporation line for lake waters reported in Diefendorf and Patterson (2005). (C) monthly variations in $\delta^{18}O$ of Carran rainfall and Lough Gealáin lake water. (D) Variation in $\delta^{18}O$ with depth in Lough Gealáin. [Color figure can be viewed at wileyonlinelibrary.com]
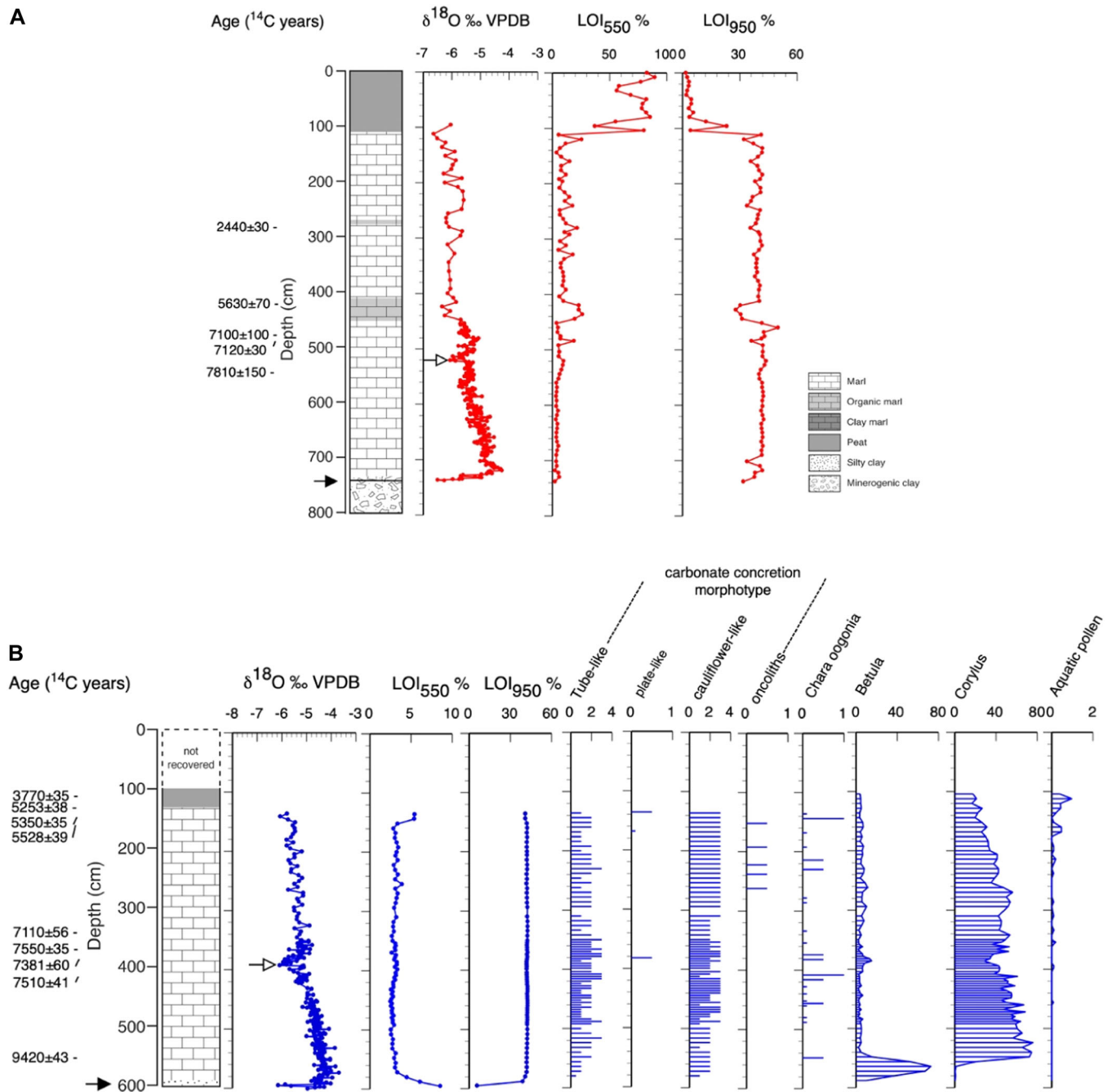
Figure 3. Lithostratigraphy, radiocarbon dates, oxygen-isotope and other data from the Burren lakes. (A) Records from Lough Avolla core LA2B. (B) Records from Lough Gealáin core MLM8. Pollen data are percentages based on a sum of total terrestrial pollen and fern spores. Carbonate concretion morphotype occurrences and Characeae oogonia records are semi-quantitative categorical measures of abundance: 0.25 = single occurrence; 0.5 = rare; 1 = occasional; 2 = frequent; 3 = abundant. For both sequences, only those radiocarbon dates used in age modelling are shown. In both panels, open arrows mark levels of the negative isotope excursion associated with the Early Holocene cooling event around 8.2 cal ka BP and the filled arrows mark the transition from minerogenic sediment to marl that is taken to represent the onset of the Holocene. See text for further explanation. For a full list of radiocarbon dates, see Table 1. [Color figure can be viewed at wileyonlinelibrary.com]

obtained for the core of which five were used in the age–depth model (Table 1) (Fig. 4). In addition, the negative $\delta^{18}O_{CaCO3}$ excursion centred on 520 cm in LA2B was assumed to be the time-equivalent of the similar excursion at 386 cm depth in MLM8 (Fig. 3), dated to 8240 cal a BP. A calendar age of 8240 cal a BP at 520 cm was therefore included in the LA2B age model, as discussed in Holmes et al. (2016). Two of the four radiocarbon dates (at 713 and 500.5 cm depth) appear much too young when compared with the other chronological information, and are therefore rejected, although we have no firm explanation for why they might be outliers. The dates at 501.5 and 468.5 cm, whilst broadly consistent with age–depth relationships, form age inversions and they are therefore also excluded from the age–depth

model for LA2B. We further note that the exclusion of these two dates provides a much better age alignment of the negative $\delta^{18}O_{CaCO3}$ excursion with that in MLM8.

Lake-sediment oxygen isotopes

Carbonate oxygen isotope values ($\delta^{18}O_{CaCO3}$) for MLM8 cover the section from 602 to 136 cm (Fig. 3). Minimum values around −6‰ close to the base preceded a sharp rise to around −4‰, followed by a gradual decline to about −6‰ in the uppermost levels analysed. A sharp negative excursion, marked by two phases separated by slightly more positive values, is centred on 387 cm. $\delta^{18}O_{CaCO3}$ values for LA2B extend from 738 to 96 cm

Table 1. Radiocarbon dates from cores MLM8 and LA2B

| Core	Depth (cm)	Laboratory reference	Material	Radiocarbon age (^{14}C a BP)	Calibrated age range (95%) (cal a BP)
MLM8	104.5	SUERC-13608*	Charcoal, *Carex* seeds	3770 ± 35	3993–4243
MLM8	129.5	SUERC-19462*	*Betula* bud scales	5253 ± 38	5926–6178
MLM8	137.5	SUERC-20023	Bud scales and charred fragments	5350 ± 35	6002–6770
MLM8	139.5	SUERC-19463	Charcoal fragments	5528 ± 39	6281–6401
MLM8	339.5	SUERC-13865	Bud scales, fragments of indet. leaf charcoal and charred moss fragments	7110 ± 56	7829–8024
MLM8	375.5	SUERC-20024	*Betula* bud scales	7550 ± 35	8326–8414
MLM8	383.5	SUERC-13866	Bud scales and small charcoal fragments	7381 ± 60	8046–8339
MLM8	409.5	SUERC-19464	Pine needle fragments, *Betula* bud scales	7510 ± 41	8206–8402
MLM8	546.5	SUERC-13609	Leaf fragment,?*Corylus*	9420 ± 43	10525–10755
LA2B	280.5	Poz-35347	Plant matter	2440 ± 30	2357–2700
LA2B	419	Beta-168919	Bulk organic matter	5630 ± 70	6291–6600
LA2B	468.5	Poz-31228*	Plant matter	7860 ± 80	8481–8986
LA2B	469.5	Poz-31719	Twig + Campanulaceae seed	7100 ± 100	7714–8157
LA2B	475	Poz-31229	Campanulaceae seed	7120 ± 80	7788–8157
LA2B	500.5	Poz-31230*	Plant matter	1230 ± 30	1069–1261
LA2B	501.5	Poz-31720*	Plant matter	7880 ± 40	8586–8971
LA2B	544.5	Poz-31232	Plant matter + charcoal fragment	7810 ± 150	8368–9015
LA2B	713	Poz-35348*	Plant matter	320 ± 30	305–465

*Excluded from age–depth model.
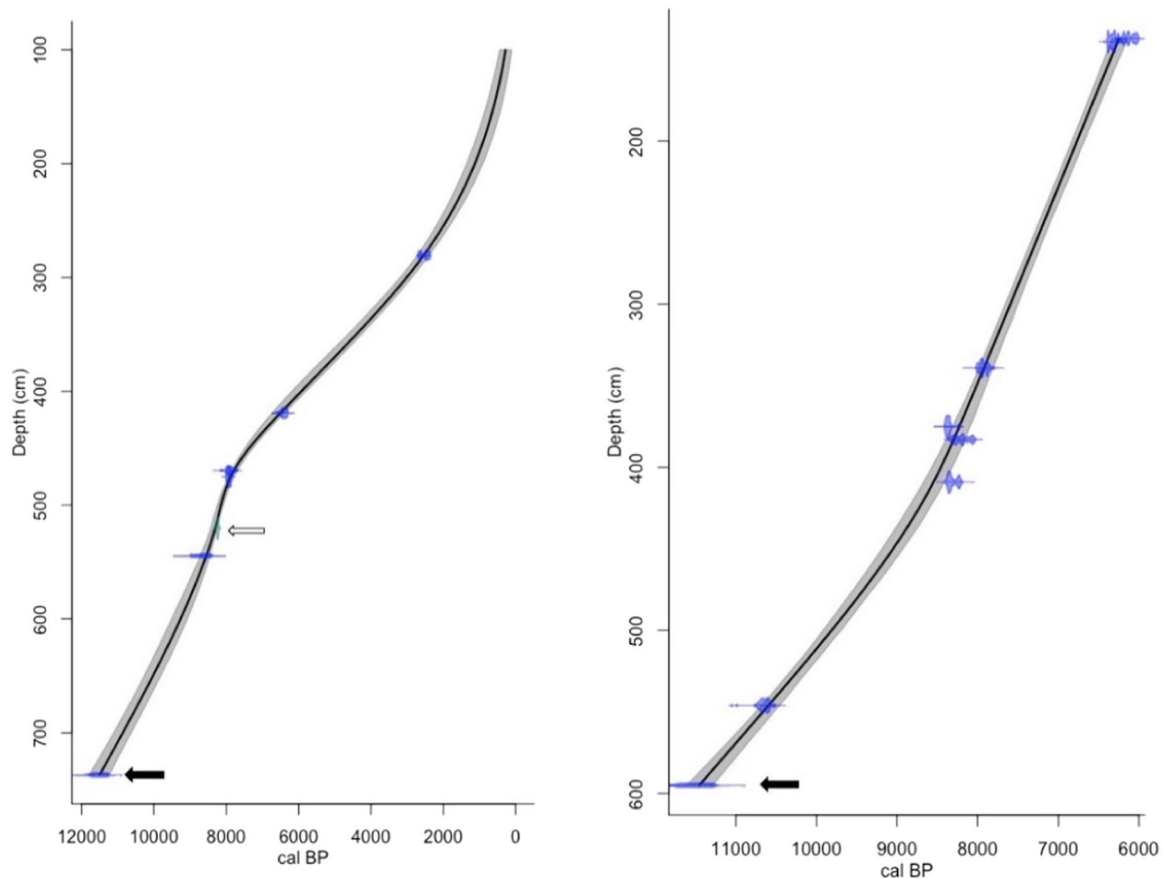
Figure 4. Age–depth models using a smooth spline for LA2B (left) and MLM8 (right). Filled arrows represent the depth of the transition from minerogenic sediment to marl in both cores. Open arrow in LA2B represents the depth of the negative $\delta^{18}O_{CaCO3}$ excursion that is assumed to correlate with a similar excursion in MLM8 (Fig. 3). Shading represents 96% confidence intervals. [Color figure can be viewed at wileyonlinelibrary.com]

(Fig. 3). There is a sharp rise in $\delta^{18}O_{CaCO3}$ from −7.54‰ at 738 cm to −4.26‰ at 720 cm, followed by a steady decline to around −6‰ at 400 cm and a further decline to about −6.5‰ above this, in similar fashion to MLM8: analyses were undertaken at lower stratigraphical resolution above 454 cm. Several negative excursions centred on 520, 430 and 260 cm are superimposed on the general trend (Fig. 5).

The oxygen-isotope values for MLM8 are generally ^{18}O-enriched by ~0.5 to 1‰ compared to LA2B for much of the interval from 11.6 to 6.5 cal ka BP: undue significance should not be attributed to variations in the differences at subcentennial timescales, owing to uncertainties in chronology at the decadal scale. Values for the two sequences converge between 8.7 and 7.8 cal ka BP, a time interval centred on the 8.2 cal ka BP event, which
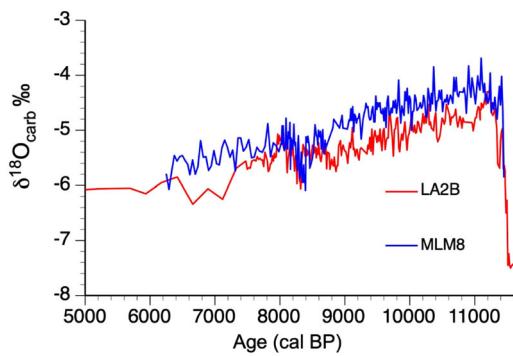
Figure 5. Oxygen-isotope records from Lough Gealáin core MLM8 and Lough Avolla Core LA2B versus age for the interval 11–5 cal ka BP (LA2B) or 6 cal ka BP (MLM8). [Color figure can be viewed at wileyonlinelibrary.com]

is clearly registered in both isotope sequences (Holmes et al., 2016). After 7.8 cal ka BP, the two records seem to diverge once more, with values from MLM8 more ^{18}O-enriched, as for the earlier parts of the records, although there are too few datapoints from MLM8 to confirm this.

There is a rapid rise in the carbonate content and decline in organic carbon [inferred from loss-on-ignition (LOI) in MLM8 in the earliest part of the sequence, at the start of the Holocene, whereas carbonate values are high and organic carbon values low at the start of the Holocene in LA2B (Fig. 3). In both cores, high carbonate and low organic carbon characterize much of the sequences, although there are minor changes in LA2B midway through the core, beginning at about 450 cm, and a sharp fall in carbonate in the uppermost peat (the peat was not analysed for LOI in MLM8). Despite these details, both basins supported marl-precipitating lakes for most of the Holocene. Carbonate concretions in MLM8 were dominated by tube-like and cauliflower-like forms, with only occasional occurrences of other types (Fig. 3). Key changes in pollen in MLM8 include the rise in *Betula* pollen close to the start of the Holocene with *Corylus* pollen increasing sharply at around 10.7 cal ka BP and remaining at high levels for the remainder of the record. Aquatic pollen appears in MLM8 shortly before 9.2 cal ka BP and becomes more common after ~8 cal ka BP. *Chara* oogonia are present consistently after about 9.5 cal ka BP in MLM8 (Fig. 3).

Model results

For the comparison of the lake-sediment data with the model, we focus on differences between the Early and Mid-Holocene, defined as 11–9 and 7–5 cal ka BP, respectively, acknowledging that for the interval 6–5 cal ka BP, we only have data for one of the lake sites. Modelled changes during the transition from the end of the Younger Dryas stadial into the Holocene are also not considered because the Younger Dryas forcing was not included, meaning that the simulation for 12–11 cal ka BP is unlikely to be realistic. The model results are also unable to simulate the short-lived 8.2 cal ka BP event. Modelled $\delta^{18}O_{ppt}$ shows marked changes over Europe and the North Atlantic during the Early to Mid-Holocene (Fig. 6). For the grid square considered in this study, weighted average $\delta^{18}O_{ppt}$ was about −6.6‰ at 11 cal ka BP, −7.4 at 8 cal ka BP and −7.2‰ at 6 cal ka BP.

Discussion

The lake-isotope records show remarkable similarity for the period from 11.6 to 6 cal ka BP, for which we have data from both sites. We conclude that they represent regional, rather

than basin-specific, signatures and therefore discuss them together, highlighting differences where relevant. The key common features of the two records are (i) the sharp rise in $\delta^{18}O$ values at their starts, (ii) the peaks in $\delta^{18}O$ values that occur shortly after the start of the Holocene, around 11.6 cal ka BP, and (iii) the steady ~2‰ decrease in $\delta^{18}O$ from the peak up to the Mid-Holocene. The ~180-year ~1‰ negative $\delta^{18}O$ excursion in the Early Holocene associated with the 8200-year cooling event is also seen in both records (Holmes et al., 2016), but is not discussed in this study. The main difference between the two records is the ~0.5‰ ^{18}O enrichment that is seen in MLM8 compared with LA2B prior to 8.6 cal ka BP.

The rise in oxygen-isotope values at the start of both sequences is consistent with the transition from the end of the Younger Dryas Stadial into the earliest Holocene. We focus our attention on the most striking feature of the longer-term trend, namely the steady ~2‰ decrease in $\delta^{18}O_{CaCO3}$ from just after the start of the Holocene until ~5 to 6 cal ka BP. The fact that this trend is clearly replicated in the two lake-sediment records from the Burren suggests that it was driven by regional hydroclimate and not by basin-specific factors. A decrease in the $\delta^{18}O_{CaCO3}$ over this interval could in principle have been caused by (i) an increase in the calcification season (i.e. spring–summer) water temperature, which would decrease the fractionation of ^{18}O between calcite and water by about 0.2‰ °C^{-1} and/or (ii) a decrease in the $\delta^{18}O$ of lake water, which could have multiple potential causes. We discuss the relative importance and implications of these controls below.

A decrease in $\delta^{18}O_{CaCO3}$ of about 2‰ is unlikely to be the result of water temperature change, since this would require a warming >8.5 °C between the Early and Mid-Holocene, even assuming that any changes in water temperature were unaccompanied by shifts in air temperature, which would impact the $\delta^{18}O$ of precipitation in the opposite direction. Various palaeotemperature proxies indicate that warm-season temperatures during the Early Holocene were only slightly lower than those in the Mid-Holocene.

There is no clear evidence in the pollen data from Lough Gealáin for significant long-term changes in temperature in the Early to Mid-Holocene. The sharp increase in *Corylus* between the start of the MLM8 sequence and about 10.7 cal ka BP (Fig. 3) could indicate amelioration and then stabilization of temperature in the very earliest part of the Holocene (Tallantire, 2002) but may also be related to vegetation succession at this time (Ahlberg et al., 2001). Evidence for only slightly cooler summers over Britain and Ireland at the opening of the Holocene is also seen in chironomid-inferred temperature records (Dalton et al., 2005; Lang et al., 2010; McKeown et al., 2019). Regional reconstructions support this. Compilations of pollen data (Mauri et al., 2015) indicate that summer (JJA) temperatures over NW Europe were up to ~0.5 °C lower than pre-industrial at 11 cal ka BP, rising to up to 1 °C higher by 9 cal ka BP, and between 1 and 2 °C higher by the Mid-Holocene (~6 cal ka BP). In contrast, pollen-inferred winter (DJF) temperatures were ≤5 °C lower than pre-industrial around 11 cal ka BP rising steadily through the Holocene, but not reaching pre-industrial values until ~2 cal ka BP (Mauri et al., 2015). Of course, lowered Early Holocene water temperature would have been accompanied by reduced air temperature, as the two would not vary independently in the present setting: all other things remaining equal, reduced air temperature would have been accompanied by lower $\delta^{18}O_{ppt}$, which would in turn lower $\delta^{18}O_{lake}$.

The major trends in $\delta^{18}O_{CaCO3}$ in these two Irish lakes are therefore unlikely to have been a direct result of temperature change but are instead much better explained primarily by changes in $\delta^{18}O_{lake}$. Changes in $\delta^{18}O_{lake}$ could have been
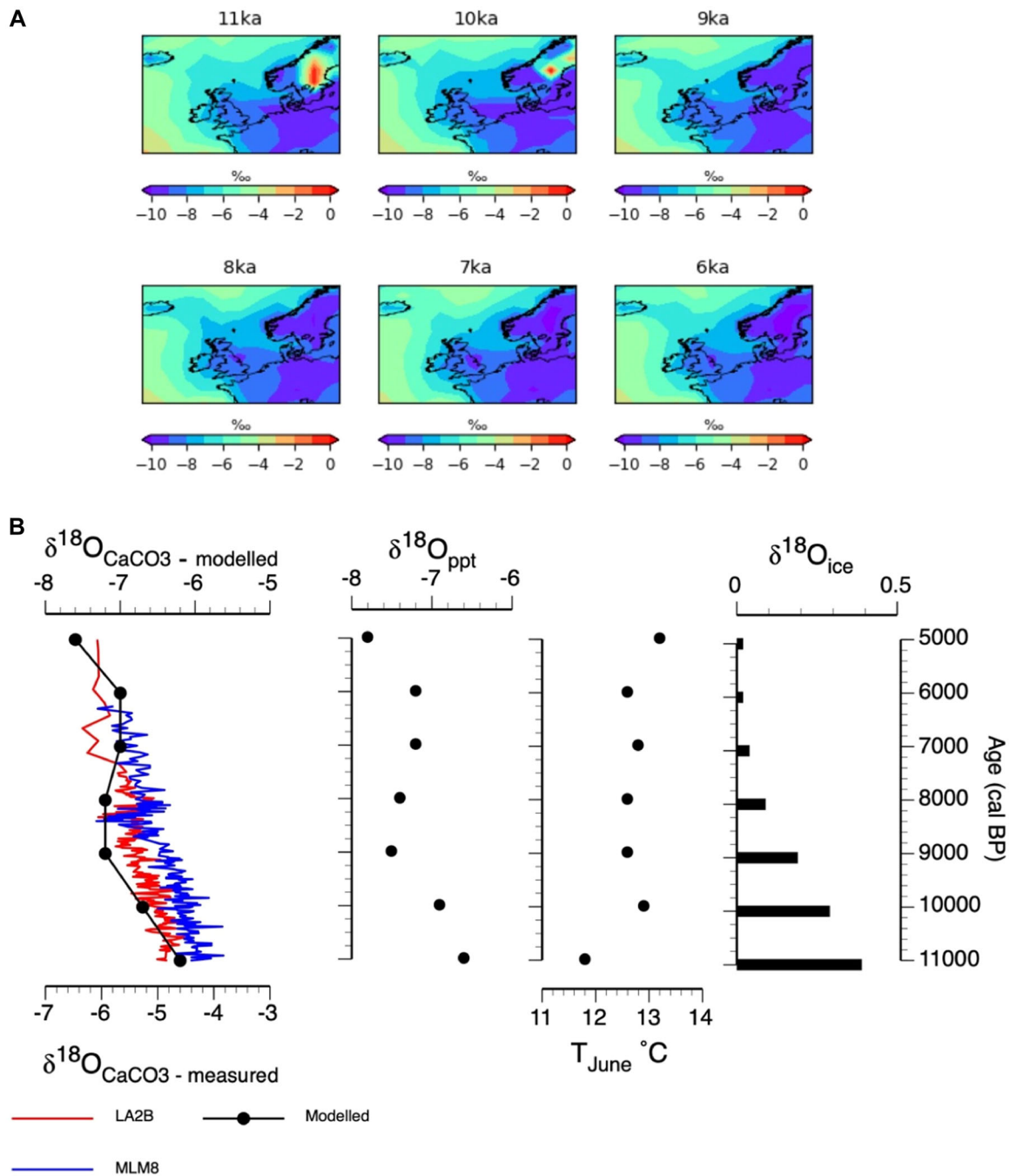
Figure 6. (A) $\delta^{18}O_{ppt}$ values from 1000-year snapshot experiments with iHadCM3 from 11 to 6 cal ka BP. (B) Comparison of measured and modelled $\delta^{18}O_{CaCO3}$ values from the lake records, modelled $\delta^{18}O_{ppt}$, and summer temperature and ice-volume corrections ($\delta^{18}O_{ice}$) applied to the $\delta^{18}O_{ppt}$ values for each timeslice. Modelled values of weighted annual $\delta^{18}O_{ppt}$ and summer temperature are for the grid square coordinates 52.5°N, 11.25°W. The $\delta^{18}O_{CaCO3}$ values were calculated using the equation of Kim and O'Neil (1997) using modelled $\delta^{18}O_{ppt}$ and modelled summer (June) temperature. [Color figure can be viewed at wileyonlinelibrary.com]

caused by a decrease in the $\delta^{18}O$ of input water or a reduction over time in evaporative enrichment of lake water. We evaluate each of these controls in turn. Evaporation leads to preferential loss of $H_2^{16}O$, enriching lake water in $H_2^{18}O$ and thus raising $\delta^{18}O_{lake}$. Long-term trends in evaporative enrichment could therefore explain changes in $\delta^{18}O_{lake}$ and in turn $\delta^{18}O_{CaCO3}$. Under present conditions, Lough Gealáin shows an ~1‰ ^{18}O enrichment compared with Carran precipitation, which is similar to Lough Avolla lake and inflow water, although as noted we have limited modern data from the latter. However, the differences between the $\delta^{18}O$ of Lough Gealáin and Carran rainfall are unlikely to be the result of evaporative enrichment (cf. Holmes et al., 2016), since the $\delta^{18}O$ values of Lough Gealáin waters do not fall on an evaporation line

(Fig. 2). Rather, they may be explained by local gradients in $\delta^{18}O_{ppt}$. Whether the $\delta^{18}O$ of the two lakes differs at present is inconclusive based on modern water isotope data, owing to the small number of measurements from Lough Avolla. However, the ~0.5‰ difference in $\delta^{18}O_{CaCO3}$ in MLM8 and LA2B for much of the records suggests that a clear difference prevailed throughout much of the Early and Mid-Holocene, perhaps reflecting $\delta^{18}O_{ppt}$ gradients between the two lakes. It is conceivable that enhanced evaporative enrichment in the Early Holocene compared to the Mid-Holocene could partly explain the overall pattern of elevated $\delta^{18}O_{CaCO3}$ values in the Early Holocene in the two records. Evaporative enrichment certainly seems to have affected Lough Gur, which lies ~65 km SSE of the Burren lakes at present (since its isotopic
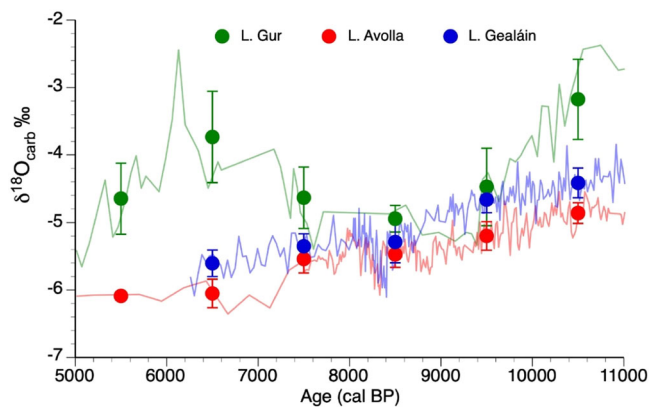
Figure 7. Early to Mid-Holocene $\delta^{18}O_{carb}$ records for Lough Gealáin, Lough Avolla (this study) and Lough Gur (Ahlberg et al., 2001: see Supporting Information for age model development). Data are also presented as mean ± 1 standard deviation $\delta^{18}O_{carb}$‰ for each 1000-year 'bin' between 11 000 and 5000 cal a BP (11 000 and 6000 cal a BP for Lough Gealáin) (filled circles and error bars) to highlight the long-term trends and allow for chronological uncertainties in the comparison of the two Burren time series, which are well aligned, with the Lough Gur record. [Color figure can be viewed at wileyonlinelibrary.com]

composition lies on a local evaporation line: Fig. 2) and during the Early to Mid-Holocene, with a $\delta^{18}O$ trend similar to that in Lough Avolla and Lough Lough Gealáin, but with isotope values up to 2‰ less negative (Ahlberg et al., 2001) (Fig. 7). However, whereas the $\delta^{18}O$ offset at Lough Gur is greatest at ~11 cal ka BP and declines thereafter, between Lough Gealáin and Lough Avolla it is constant at ~0.5‰ between 11.1 and 8.7 cal ka BP. This would be consistent with a shift in the isotopic composition of incoming precipitation rather than any within-lake evaporative effect for the latter two sites. Carbonate-grain morphology provides some support for lack of any hydrological change during this interval (Fig. 3). In temperate-region marl lakes, sediment formation and composition are linked to water depth (Murphy and Wilkinson 1980, Magny 1992, 2007) with a change in assemblage of carbonate concretions seen with depth along a littoral transect. Oncoliths are typical for near-shore environments, cauliflower-like forms for the littoral platform, plate-like concretions along the edges of the platform bench and tube-like concretions from the Characeae-dominated platform slopes, with the upper slope composed mainly of fragments of encrusted *Chara* and abundant *Chara* oogonia (sandy algal micrite facies) and the lower slope, probably below the photic zone in water depths of c. 7–10 m, being associated with only small fragments of *Chara* encrustation and abundant gastropod remains (Murphy and Wilkinson 1980). Increased presence of cauliflower-like carbonate concretions and the regular occurrence of charophyte oogonia from about 9.8 cal ka BP suggest a slight lowering of water levels in Lough Gealáin from this time although this could reflect marl-bench progression leading to lowered water levels at the core site rather than an overall lowering of lake level. In short, there is no evidence for *significant* hydrological change during this interval that would be consistent with changing evaporative enrichment.

Local palaeoecological evidence for warm-season temperatures in the Early Holocene is similarly ambivalent. On the one hand, *Najas maritima* macrofossils have been found at Red Bog near Lough Gur (Godwin 1975, p. 371) and at Gortlecka, a small lake at the foot of Mullagh Mór (Fig. 1), just above Lough Gealáin (Watts, 1984), dating to the Early Holocene. *Najas marina* is an aquatic summer annual plant that is no longer found in Ireland, its growth being constrained by late spring warming and declining light in autumn (Handley and

Davy 2005). Its presence here during the Early Holocene has been interpreted as indicating warmer summers than in recent times. On the other hand, the record of aquatic pollen and changes in carbonate content in sediments from Lough Gealáin indicate rapidly increasing water levels between c. 11 650 and 11 100 cal a BP, whereas increasing evaporation would have the opposite effect, all other things being equal. Thus, while evaporative effects may have contributed to the $\delta^{18}O$ record of western Irish lakes, we conclude that the decrease in $\delta^{18}O_{CaCO3}$ during the Early to Mid-Holocene is better explained primarily by changing $\delta^{18}O_{ppt}$.

The isotopic composition of input water to the lakes is dependent primarily on the $\delta^{18}O$ of precipitation. Although the two Burren lakes are largely groundwater fed, the isotopic composition of groundwater itself is closely linked to the isotopic composition of weighted annual precipitation, which is controlled by condensation temperature, overall rainfall amount and its seasonal distribution, and by the source, transport pathway and rainout history of the moisture-bearing air mass, or more broadly to atmospheric circulation. As noted above, there is no clear evidence for a temperature change over Ireland in the Early to Mid-Holocene of around 4 °C that would be required to explain the reduction of $\delta^{18}O_{CaCO3}$, given the opposing impacts of temperature change on the $\delta^{18}O$ of precipitation and on calcite water fractionation. An increase in rainfall amount between the Early and Mid-Holocene could conceivably have caused a reduction in the $\delta^{18}O$ of precipitation. However, as noted above there is no palaeohydrological evidence for such a change in the Burren or more widely (Mauri et al., 2015). Changes in the seasonal distribution of precipitation can potentially impact the weighted mean $\delta^{18}O$ of precipitation without any change in annual rainfall amount, since the $\delta^{18}O_{ppt}$ differs monthly (Fig. 2). A change to more negative values in rainfall from this mechanism would imply an increase in winter rainfall: for example, Candy et al. (2015) have previously suggested that an increase in the proportion of annual rainfall in winter could explain Holocene patterns of $\delta^{18}O_{CaCO3}$ in Britain. However, large and probably unrealistic changes in the seasonal distribution of precipitation would be required to explain the ~2‰ decline in $\delta^{18}O_{CaCO3}$ seen in the Burren records.

Event-based investigations of the oxygen-isotope composition of rainfall over Britain and Ireland suggest that $\delta^{18}O_{ppt}$ is not a simple function of air temperature or rainfall amount, but rather a response to changes in atmospheric circulation (Baldini et al., 2010; Tyler et al., 2016). Although Baldini et al. (2010) found considerable overlap in the isotopic composition of Irish rainfall derived from different sources, they noted that moisture from southerly or northerly derived events was about 2‰ more negative than moisture derived from the west. However, they further concluded that large, prolonged changes in atmospheric circulation would be required to register in Irish palaeo-isotope records. Consequently, if the Early Holocene ~2‰ decrease in $\delta^{18}O_{CaCO3}$ is to be explained by changes in air-mass source and trajectory, substantial changes in atmospheric circulation must have occurred. Finally, changes in the isotopic composition of the North Atlantic Ocean (the oxygen-isotope composition of seawater, $\delta^{18}O_{sw}$), the original source of atmospheric vapour from which Irish precipitation is formed, will also impact $\delta^{18}O_{ppt}$. During the Early to Mid-Holocene, the melting of the Laurentide ice sheet led to a small but significant decrease in $\delta^{18}O_{sw}$.

Previous reports of European Holocene oxygen-isotope records have invoked atmospheric circulation to explain observed changes. Hammarlund et al. (2002) reported similar trends in Holocene oxygen-isotope values in Lake Tibetanus,
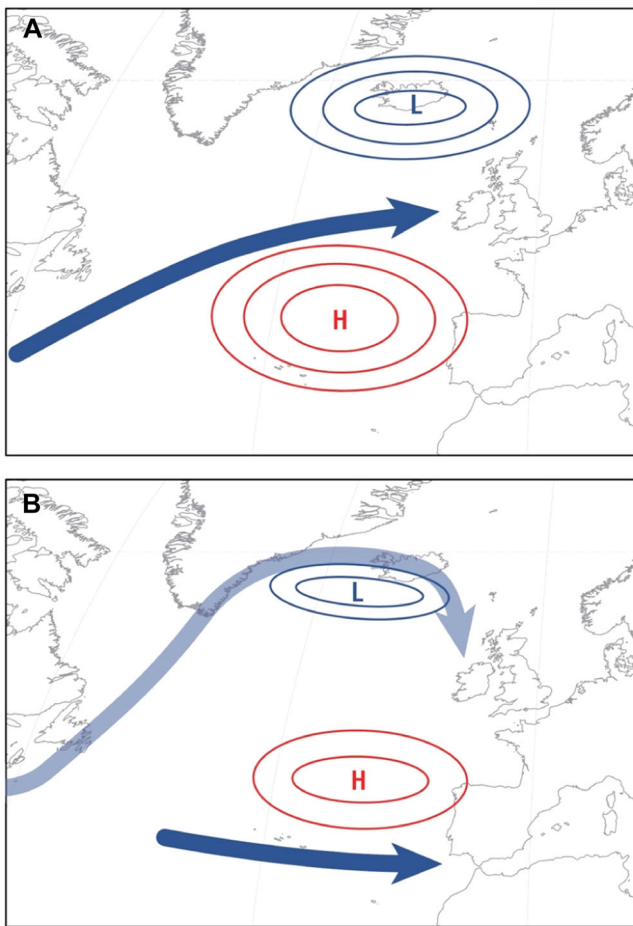
Figure 8. Cartoon representing possible atmospheric circulation during (A) the Early Holocene and (B) the Mid-Holocene to explain trends in carbonate oxygen isotope values in the lakes in this study and in northern Sweden (in Hammarlund et al., 2002). H and L = high and low surface pressure, respectively. Blue arrows mark the approximate position and strength (dark blue = stronger, light blue = weaker) of the jet stream in the upper atmosphere, and trajectory of storm tracks. [Color figure can be viewed at wileyonlinelibrary.com]

from coastal Denmark over the past 10 kyr. Although storminess is linked to NAO behaviour, they suggested that the relationship may be more complex and identified millennial-scale storminess episodes in both the Early and Mid-Holocene, although the period between 9 and 10 cal ka BP being generally less stormy than the Mid-Holocene. They suggested that millennial-scale storminess is driven by ocean circulation and noted that the subpolar gyre (SPG) was weakened in the Early Holocene according to the record of Thornalley et al. (2009), although this record of SPG strength has been disputed and SPG was probably actually stronger in the Early Holocene (Gregoire et al., 2018; D. Thornalley, pers. comm, 2020). In short, although there is evidence for changing atmospheric circulation during the Early to Mid-Holocene, empirical evidence provides a conflicting picture of the details of those changes.

Results from the 1000-year snapshot experiments using iHadCM3 were used here to further investigate the patterns of $\delta^{18}O_{CaCO3}$ in the Irish lakes over the Early to Mid-Holocene (Fig. 6). For the grid box used here, the modelled value of weighted $\delta^{18}O_{ppt}$ was −6.6‰ at 11 cal ka BP, falling to −7.2‰ by 6 cal ka BP and −7.8‰ by 5 cal ka BP, with an 11–5 cal ka BP difference of 1.2‰. Modelled summer temperature and weighted $\delta^{18}O_{ppt}$ values from iHadCM3 can be used to approximate the lake $\delta^{18}O_{CaCO3}$ values (Fig. 8) assuming (i) that lacustrine carbonate precipitated in summer, (ii) $\delta^{18}O_{lake-water}$ approximated weighted annual $\delta^{18}O_{ppt}$ and (iii) carbonate precipitated in isotopic equilibrium with lake water. The weighted annual $\delta^{18}O_{ppt}$ value for Carran of −6‰ VSMOW and a mean June temperature of ~13 °C yields a $\delta^{18}O_{CaCO3}$ value of −5.9‰ VPDB, close to modern carbonate values of −5.4 ± 0.2‰ VPDB ($n = 3$) in Lough Avolla and −5.2 ± 0.2‰ ($n = 5$) VPDB in Lough Gealáin, suggesting that these assumptions are reasonable. Modelled $\delta^{18}O_{CaCO3}$ values were around −6.2‰ at 11 cal ka BP, falling to −7.7 by 5 cal ka BP, a reduction of 1.5‰. The modelled reduction compares well with the fall of about 1.3‰ in the lake records over the same interval (Fig. 6). However, the absolute values are up to about 2‰ more negative in modelled calcite than in the core records, probably explained by $\delta^{18}O_{ppt}$ that is more negative in the model than reality. This is not unexpected however, given the low spatial resolution of the model grid squares coupled with the large present-day gradients in the $\delta^{18}O$ values of precipitation and groundwater across Ireland and the UK (Darling et al., 2003; Baldini et al., 2010; Tyler et al., 2016). Despite the difference in the absolute $\delta^{18}O$ values between the lake-sediment data and the modelled record, the similarity in the magnitude of the trends allows us to use the model to help investigate the potential drivers of the ~1.3‰ decrease in $\delta^{18}O_{CaCO3}$ in the sediment cores. Most of the fall in $\delta^{18}O_{CaCO3}$ between the 11 and 6 cal ka BP time slices is attributed to changing values of $\delta^{18}O_{ppt}$. For the model grid square used here, 1.2‰ of a 1.5‰ shift (80%) is due to changing isotope values of precipitation, as noted above; modelled weighted annual $\delta^{18}O_{ppt}$ was −6.6‰ at 11 cal ka BP, −7.4‰ at 8 cal ka BP and −7.2‰ at 6 cal ka BP: the remainder being explained by higher Mid-Holocene June temperatures (~0.8 °C higher at 6 cal ka BP than at 11 cal ka BP) (Fig. 6). This drop in $\delta^{18}O_{ppt}$ in the model is nearly all explained by the change in $\delta^{18}O_{SW}$ that has been applied, from the melting of ice sheets between 11 and 6 cal ka BP; that is, to a change in the $\delta^{18}O$ of source water, although a small residual component may relate to a shift in source water location or the transport pathway of water vapour from source to Ireland.

The overall pattern of modelled and measured $\delta^{18}O_{CaCO3}$ values for the Irish lake sites agrees quite well over the Early to Mid-Holocene. However, the explanation for this change – a decrease in $\delta^{18}O_{ppt}$ over the same period caused mainly by a

northern Sweden, to those observed in Ireland in this study, and attributed the elevated values to decreased distillation of moisture as air masses crossed the Scandes Mountains, as a result of strengthened westerlies during the Early Holocene associated with a more zonal atmospheric circulation. This scenario is broadly analogous to NAO-positive (Fig. 8). Similar patterns of oxygen-isotope variations in northern Scandinavian speleothems lend support to this interpretation (Hammarlund and Edwards, 2008). Hammarlund et al. (2002) regarded the effect of changing $\delta^{18}O_{sw}$ as insignificant.

In contrast, Baker et al. (2017) interpreted lower Early–Holocene $\delta^{18}O_{CaCO3}$ values in a speleothem from the Urals as indicative of enhanced atmospheric blocking, which they attributed to the impact of the remnant Laurentide ice sheet. Blocking leads to more meridional airflow and hence lower $\delta^{18}O_{ppt}$ and is broadly analogous to NAO-negative. Wassenburg et al. (2016) inferred a shift in NAO-type behaviour sometime after around 9 cal ka BP based on paired speleothem records from NW Africa and Europe: during the Early Holocene, NAO behaviour may have been modulated as a result of the effects of the remnant Laurentide ice sheet and associated meltwater effects, leading to a more pronounced Atlantic multidecadal oscillation (AMO) and, in turn, either to a northward shift in the westerlies or more persistent south-westerly winds. Goslin et al. (2018) noted centennial- to millennial-scale storminess episodes

reduction of $\delta^{18}O_{SW}$ due to the melting of ice sheets – is at variance with the mechanism proposed by Hammarlund et al. (2002) and Hammarlund and Edwards (2008), which attributed elevated Early Holocene $\delta^{18}O_{CaCO3}$ values in northern Scandinavia to stronger westerly airflow, associated with reduced moisture distillation as air masses passed over the upwind Scandes Mountains. In other words, the $\delta^{18}O_{CaCO3}$ values were explained by $\delta^{18}O_{ppt}$ and, in turn, changed atmospheric circulation (Fig. 8). Enhanced zonal circulation could also explain the pattern of $\delta^{18}O_{CaCO3}$ values in the Irish sites. However, Ireland lacks the strong topographic barrier of the Scandes Mountains present in northern Scandinavia (the Burren uplands, which lie upwind of the lake sites in Ireland, only rise to around 200–300 m a.s.l.) so if this explanation is correct, the mechanism must have operated in the absence of significant topographic control. Edwards et al. (1996) showed a similar pattern of inferred $\delta^{18}O_{ppt}$ from lakes in Canada to the records in Ireland and northern Scandinavia, and also attributed this pattern to enhanced zonal circulation in the Early Holocene. The Canadian sites are upwind of the North Atlantic, and so it is unlikely that a change in $\delta^{18}O_{SW}$ could explain the pattern here. Reconstructions of $\delta^{18}O_{SW}$ for the Holocene, although limited in number, indicate that values varied spatially (Waelbroeck et al., 2014), as for present (LeGrande and Schmidt, 2006). Given this and a lack of information about possible changes in the location of the source of precipitation to Europe during the Holocene, the contribution of changing $\delta^{18}O_{SW}$ to the patterns of $\delta^{18}O_{CaCO3}$ values in our Irish lakes remains uncertain.

Conclusions

Lake-sediment carbonate isotope records from the two neighbouring lakes in western Ireland, which are presented here, show consistent patterns of change during the Early and Mid-Holocene, suggesting that they are responding to regional hydroclimate rather than site-specific factors, with changes in the oxygen-isotope composition of precipitation inferred to have been the dominant control. Comparison of the lake-sediment records with outputs from iHadCM3, an isotope-enabled GCM, indicates that the decline in $\delta^{18}O_{CaCO3}$ values between the start of the Holocene and ~6 cal ka BP can be explained mainly by a decrease in the $\delta^{18}O$ of the ocean source water, with melting of the Laurentide ice sheet. A small component of the $\delta^{18}O_{CaCO3}$ change in the model may be the result of a shift in the transport pathways of moisture over this period. Although the model suggests that increased zonal airflow, and hence less distilled moisture, during the Early Holocene is not required to explain the elevated Early Holocene $\delta^{18}O_{CaCO3}$ values, this seems unlikely given similar patterns in lake-sediment records from upwind locations. In short, although the model seems to agree quite well with the lake isotope records, this may not necessarily be for the same reasons. The location of the two Irish lakes, very close to the western extreme of Europe, may make these sites especially sensitive to the isotopic composition of ocean water although the patterns of change are also consistent with enhanced zonal circulation in the Early Holocene too. Patterns of $\delta^{18}O_{CaCO3}$ contrast markedly with published patterns of Early to Mid-Holocene temperature reconstructed using a range of proxies, indicating that the isotopic record in the Irish lakes is not a direct proxy for temperature over this time interval. Further investigation of possible changes in atmospheric circulation over Europe during the Holocene will require examination of isotope records from a much more extensive set of sites across the region and could utilize isotope data from lake sediments and from other archives, notably speleothems.

Declaration of competing interest

The authors declare that they have no known competing financial interests or personal relationships that could have appeared to influence the work reported in this paper.

Author contributions—J.H. designed the study, oversaw the isotope analyses and produced the initial draft. J.T. and M.H. were responsible for the GCM modelling and M.J. undertook forward modelling of the lake-sediment isotope record. N.R. was responsible for core recovery and water sampling from Lough Avolla and for the sediment analyses of LA2B. I.F. undertook pollen and sediment analyses from MLM8. All authors contributed to drafting of the manuscript.

Data availability statement

Monitoring and lake-sediment data are available from the UK NERC RAPID Data centre (https://www.bodc.ac.uk/projects/data_management/uk/rapid/data_inventories/palaeo_sampling/isomap-uk/).

Supporting information

Additional supporting information can be found in the online version of this article.

Abbreviations. AMO, Atlantic Multi-decadal Oscillation; AMS, accelerator mass spectrometry; DJF, December–January–February; GNIP, Global Network of Isotopes in Precipitation; HadCM3, Hadley Centre Coupled Model, version 3; IAEA, International Atomic Energy Agency; iHadCM3, isotope-enabled version of HadCM3; JJA, June–July–August; LMWL, local meteoric water line.; LOI, loss on ignition; NAO, North Atlantic Oscillation; VPDB, Vienna PeeDee Belemnite; VSMOW, Vienna Standard Mean Ocean Water; WMO, World Meteorological Organization.

References

Ahlberg, K., Almgren, E., Wright, Jr., H.E. & Ito, E. (2001) Holocene stable-isotope stratigraphy at Lough Gur, County Limerick, Western Ireland. *The Holocene*, 11, 367–372.

Baker, J.L., Lachniet, M.S., Chervyatsova, O., Asmerom, Y. & Polyak, V.J. (2017) Holocene warming in western continental Eurasia driven by glacial retreat and greenhouse forcing. *Nature Geoscience*, 10, 430–435.

Baldini, L.M., McDermott, F., Baldini, J.U.L., Fischer, M.J. & Möllhoff, M. (2010) An investigation of the controls on Irish precipitation $\delta^{18}O$ values on monthly and event timescales. *Climate Dynamics*, 35, 977–993.

Blaauw, M. (2010) Methods and code for 'classical' age-modelling of radiocarbon sequences. *Quaternary Geochronology*, 5, 512–518.

Bova, S., Rosenthal, Y., Liu, Z., Godad, S.P. & Yan, M. (2021) Seasonal origin of the thermal maxima at the Holocene and the last interglacial. *Nature*, 589, 548–553.

Candy, I., Farry, A., Darvill, C.M., Palmer, A., Blockley, S.P.E., Matthews, I.P. et al. (2015) The evolution of Palaeolake Flixton and the environmental context of Star Carr: an oxygen and carbon isotopic record of environmental change for the early Holocene. *Proceedings of the Geologists' Association*, 126, 60–71.

Carlson, A.E., LeGrande, A.N., Oppo, D.W., Came, R.E., Schmidt, G.A., Anslow, F.S. et al. (2008) Rapid early Holocene deglaciation of the Laurentide ice sheet. *Nature Geoscience*, 1, 620–624.

Coleman, M.L., Shepherd, T.J., Durham, J.J., Rouse, J.E. & Moore, G.R. (1982) Reduction of water with zinc for hydrogen isotope analysis. *Analytical Chemistry*, 54, 993–995.

Dalton, C., Birks, H.J.B., Brooks, S.J., Cameron, N.G., Evershed, R.P., Peglar, S.M. et al. (2005) A multi-proxy study of lake-development in response to catchment changes during the Holocene at Lochnagar, north-east Scotland. *Palaeogeography, Palaeoclimatology, Palaeoecology*, 221, 175–201.

Dansgaard, W. (1964) Stable isotopes in precipitation. *Tellus*, 16, 436–468.

Darling, W.G., Bath, A.H. & Talbot, J.C. (2003) The O and H stable isotope composition of freshwaters in the British Isles. 2, surface waters and groundwater. *Hydrology and Earth System Sciences*, 7, 183–195.

Diefendorf, A.F. & Patterson, W.P. (2005) Survey of stable isotope values in Irish surface waters. *Journal of Paleolimnology*, 34, 257–269.

Drew, D. (1988) The hydrology of the upper Fergus River catchment. County Clare. *Proc. Univ. Bristol Speleol. Soc.* 18, 265–277.

Edwards, T.W.D., Wolfe, B.B. & MacDonald, G.M. (1996) Influence of changing atmospheric circulation on precipitation $\delta^{18}O$-temperature relations in Canada during the Holocene. *Quaternary Research*, 46, 211–218.

Einsiedl, F. (2012) Sea-water/groundwater interactions along a small catchment of the European Atlantic coast. *Applied Geochemistry*, 27, 73–80.

Epstein, S. & Mayeda, T. (1953) Variation of O^{18} content of waters from natural sources. *Geochimica et Cosmochimica Acta*, 4, 213–224.

Erb, M.P., McKay, N.P., Steiger, N., Dee, S., Hancock, C., Ivanovic, R.F. et al. (2022) Reconstructing Holocene temperatures in time and space using paleoclimate data assimilation, EGUsphere [preprint]. https://doi.org/10.5194/egusphere-2022-184

Feeser, I. (2009) Palaeological investigations towards reconstruction of Holocene environmental change in the Burren, Co. Clare, with particular reference to Mullach Mor and selected Burren uplands. PhD Thesis, NUI, Galway

Gaffney, F.X. (2006) Climate of Galway 1966–2005. Measurement of temperature, sunshine and rainfall. Department of Experimental Physics.

Gibbard, P.L. & Head, M.J. (2020) Chapter 30—The Quaternary Period. In: Gradstein, F. M., Ogg, J. G., Schmitz, M. D. & Ogg, G. M. (Eds) *Geologic Time Scale* 2020, Elsevier, pp. 1217–1255.

Godwin, H. (1975) *The History of the British flora*, 2nd ed. Cambridge: Cambridge University Press.

Gordon, C., Cooper, C., Senior, C.A., Banks, H., Gregory, J.M., Johns, T.C. et al. (2000) The simulation of SST, sea ice extents and ocean heat transports in a version of the Hadley centre coupled model without flux adjustments. *Climate Dynamics*, 16, 147–168.

Goslin, J., Fruergaard, M., Sander, L., Gałka, M., Menviel, L., Monkenbusch, J. et al. (2018) Holocene centennial to millennial shifts in North-Atlantic storminess and ocean dynamics. *Scientific Reports*, 8, 12778. Available at https://doi.org/10.1038/s41598-018-29949-8

Gregoire, L.J., Ivanovic, R.F., Maycock, A.C., Valdes, P.J. & Stevenson, S. (2018) Holocene lowering of the Laurentide ice sheet affects North Atlantic gyre circulation and climate. *Climate Dynamics*, 51, 3797–3813.

Hammarlund, D., Barnekow, L., Birks, H.J.B., Buchardt, B. & Edwards, T.W.D. (2002) Holocene changes in atmospheric circulation recorded in the oxygen-isotope stratigraphy of lacustrine carbonates from northern Sweden. *The Holocene*, 12, 339–351.

Hammarlund, D. & Edwards, T.W.D. (2008) Stable isotope variations in stalagmites from northwestern Sweden document changes in temperature and vegetation during the early Holocene: a comment on Sundqvist et al. 2007a. *The Holocene*, 18(6), 1007–1008.

Handley, R.J. & Davy, A.J. (2005) Temperature effects on seed maturity and dormancy cycles in an aquatic annual, *Najas marina*, at the edge of its range. *Journal of Ecology*, 93, 1185–1193.

Heiri, O., Lotter, A.F. & Lemcke, G. (2001) Loss on ignition as a method for estimating organic and carbonate content in sediments: reproducibility and comparability of results. *Journal of Paleolimnology*, 25, 101–110.

Hertzberg, J. (2021) Palaeoclimate puzzle explained by seasonal variation. *Nature*, 589, 521–522.

Holmes, J.A., Tindall, J., Roberts, N., Marshall, W., Marshall, J.D., Bingham, A. et al. (2016) Lake isotope records of the 8200-year cooling event in western Ireland: comparison with model simulations. *Quaternary Science Reviews*, 131, 341–349.

Horita, J. & Kendall, C. (2004) Stable isotope analysis of water and aqueous solutions by conventional dual-inlet mass spectrometry. In: de Groot, P.A. (ed.) *Handbook of Stable Isotope Analytical Techniques*, Vol. 1, pp. 1–37.

IAEA/GNIP. 2014. Precipitation sampling guide http://wwwnaweb.iaea.org/napc/ih/documents/other/gnip_manual_v2.02_en_hq.pdf (accessed 28 July 2020).

IAEA/WMO. (2022) Global Network of Isotopes in Precipitation. The GNIP Database: Accessible at https://nucleus.iaea.org/wiser

Jones, M.D., Cuthbert, M.O., Leng, M.J., McGowan, S., Mariethoz, G., Arrowsmith, C. et al. (2016a) Comparisons of observed and modelled lake $\delta^{18}O$ variability. *Quaternary Science Reviews*, 131, 329–340.

Jones, M.D., Dee, S., Anderson, L., Baker, A., Bowen, G. & Noone, D.C. (2016b) Water isotope systematics: Improving our palaeoclimate interpretations. *Quaternary Science Reviews*, 131, 243–249.

Jones, M.D. & Dee, S.G. (2018) Global-scale proxy system modelling of oxygen isotopes in lacustrine carbonates: new insights from isotope-enabled-model proxy-data comparison. *Quaternary Science Reviews*, 202, 19–29.

Kaufman, D., McKay, N., Routson, C., Erb, M., Dätwyler, C., Sommer, P.S. et al. (2020) Holocene global mean surface temperature, a multi-method reconstruction approach. *Scientific Data*, 7, 201.

Kim, S.T. & O'Neil, J.R. (1997) Equilibrium and nonequilibrium oxygen isotope effects in synthetic carbonates. *Geochimica et Cosmochimica Acta*, 61, 3461–3475.

Konecky, B.L., McKay, N.P., Churakova (Sidorova), O.V., Comas-Bru, L., Dassié, E.P., DeLong, K.L. et al. (2020) The Iso2k database: a global compilation of paleo-$\delta^{18}O$ and δ^2H records to aid understanding of Common Era climate. *Earth System Science Data*, 12, 2261–2288.

Lambeck, K., Rouby, H., Purcell, A., Sun, Y. & Sambridge, M. (2014) Sea level and global ice volumes from the Last Glacial Maximum to the Holocene. *Proceedings of the National Academy of Sciences*, 111, 15296–15303.

Lang, B., Bedford, A., Brooks, S.J., Jones, R.T., Richardson, N., Birks, H.J.B. et al. (2010) Early-Holocene temperature variability inferred from chironomid assemblages at Hawes Water, northwest England. *The Holocene*, 20, 943–954.

LeGrande, A.N. & Schmidt, G.A. (2006) Global gridded data set of the oxygen isotopic composition in seawater. *Geophysical Research Letters*, 33(12), L12604. Available at https://doi.org/10.1029/2006GL026011

Leng, M., Barker, P., Greenwood, P., Roberts, N. & Reed, J. (2001) Oxygen isotope analysis of diatom silica and authigenic calcite from Lake Pinarbasi, Turkey. *Journal of Paleolimnology*, 25, 343–349.

Leng, M.J. & Marshall, J.D. (2004) Palaeoclimate interpretation of stable isotope data from lake sediment archives. *Quaternary Science Reviews*, 23, 811–831.

Liu, Z., Zhu, J., Rosenthal, Y., Zhang, X., Otto-Bliesner, B.L., Timmermann, A. et al. (2014) The Holocene temperature conundrum. *Proceedings of the National Academy of Sciences*, 111, E3501–E3505.

Magny, M. (1992) Sédimentation et dynamique de comblement dans les lacs du Jura au cours des 15 derniers millénaires. *Revue d'Archéométrie*, 16, 27–49.

Magny, M. (2007) Lake level studies. In: Elias, S.A. (Ed.), West-central-europe. *Encyclopedia of Quaternary Science*. Amsterdam: Elsevier. pp. 1389–1399.

Mannella, G., Zanchetta, G., Regattieri, E., Perchiazzi, N., Drysdale, R.N., Giaccio, B. et al. (2020) Effects of organic removal techniques prior to carbonate stable isotope analysis of lacustrine marls: A case study from palaeo-lake Fucino (central Italy). *Rapid Communications in Mass Spectrometry*, 34, Available at: https://doi.org/10.1002/rcm.8623

Marcott, S.A., Shakun, J.D., Clark, P.U. & Mix, A.C. (2013) A Reconstruction of Regional and Global Temperature for the Past 11,300 Years. *Science*, 339, 1198–1201.

Marshall, J.D., Lang, B., Crowley, S.F., Weedon, G.P., van Calsteren, P., Fisher, E.H. et al. (2007) Terrestrial impact of abrupt changes in the North Atlantic thermohaline circulation: Early Holocene, UK. *Geology*, 35(7), 639–642.

Marshall, W.A. (2002) Geochemical and palaeoecological analysis of Holocene lake sediments: Lough Avolla, SW Ireland. Unpublished M.Res. thesis, University of Plymouth, UK

Marsicek, J., Shuman, B.N., Bartlein, P.J., Shafer, S.L. & Brewer, S. (2018) Reconciling divergent trends and millennial variations in Holocene temperatures. *Nature*, 554, 92–96.

Mauri, A., Davis, B.A.S., Collins, P.M. & Kaplan, J.O. (2015) The climate of Europe during the Holocene: a gridded pollen-based reconstruction and its multi-proxy evaluation. *Quaternary Science Reviews*, 112, 109–127.

Mayewski, P.A., Rohling, E.E., Stager, J.C., Karlén, W., Maasch, K.A., Meeker, L.D. et al. (2004) Holocene climate variability. *Quaternary Research*, 62, 243–255.

McKeown, M.M., Caseldine, C.J., Thompson, G., Swindles, G.T., Ivanovic, R.F., Roland, T.P. et al. (2019) Complexities in interpreting chironomid-based temperature reconstructions over the Holocene from a lake in Western Ireland. *Quaternary Science Reviews*, 222, 105908.

Moore, P.D., Webb, J.A. & Collinson, M.E. (1991) *An illustrated guide to pollen analysis*. London: Blackwell Scientific.

Murphy, D.H. & Wilkinson, B.H. (1980) Carbonate deposition and facies distribution in a central Michigan marl lake. *Sedimentology*, 27, 123–135.

O'Connell, M. & Molloy, K. (2005) Native woodland composition and dynamics: a long-term perspective based on a Holocene pollen profile from Inis Oírr, Aran Islands, western Ireland. In: Doyle, C. & Little, D. (eds.) *Ireland's native woodlands*. Dublin: Woodlands of Ireland (on CD-ROM). pp. 20–47.

Pope, V.D., Gallani, M.L., Rowntree, P.R. & Stratton, R.A. (2000) The impact of new physical parametrizations in the Hadley centre climate model: HadAM3. *Climate Dynamics*, 16, 123–146.

Reimer, P.J., Bard, E., Bayliss, A., Beck, J.W., Blackwell, P.G., Ramsey, C.B. et al. (2013) IntCal13 and Marine13 radiocarbon age calibration curves 0–50,000 years cal BP. *Radiocarbon*, 55, 1869–1887.

Renssen, H., Seppä, H., Heiri, O., Roche, D.M., Goosse, H. & Fichefet, T. (2009) The spatial and temporal complexity of the Holocene thermal maximum. *Nature Geoscience*, 2, 411–414.

Seppä, H., Hammarlund, D. & Antonsson, K. (2005) Low-frequency and high-frequency changes in temperature and effective humidity during the Holocene in south-central Sweden: implications for atmospheric and oceanic forcings of climate. *Climate Dynamics*, 25, 285–297.

Singarayer, J.S. & Valdes, P.J. (2010) High-latitude climate sensitivity to ice-sheet forcing over the last 120 kyr. *Quaternary Science Reviews*, 29, 43–55.

Smith, A.C., Wynn, P.M., Barker, P.A., Leng, M.J., Noble, S.R. & Tych, W. (2016) North Atlantic forcing of moisture delivery to Europe throughout the Holocene. *Scientific Reports*, 6, Available at: https://doi.org/10.1038/srep24745

Street-Perrott, F.A., Holmes, J.A., Robertson, I., Ficken, K.J., Koff, T., Loader, N.J. et al. (2018) The Holocene isotopic record of aquatic cellulose from Lake Äntu Sinijärv, Estonia: Influence of changing climate and organic-matter sources. *Quaternary Science Reviews*, 193, 68–83.

Tallantire, P.A. (2002) The early-Holocene spread of hazel (*Corylus avellana* L.) in Europe north and west of the Alps: an ecological hypothesis. *The Holocene*, 12, 81–96.

Thornalley, D.J.R., Elderfield, H. & McCave, I.N. (2009) Holocene oscillations in temperature and salinity of the surface subpolar North Atlantic. *Nature*, 457, 711–714.

Tindall, J.C., Valdes, P.J. & Sime, L.C. (2009) Stable water isotopes in HadCM3: Isotopic signature of El Niño–Southern Oscillation and the tropical amount effect. *Journal of Geophysical Research*, 114(114), D04111. Available at: https://doi.org/10.1029/2008JD010825

Törnqvist, T.E. & Hijma, M.P. (2012) Links between early Holocene ice-sheet decay, sea-level rise and abrupt climate change. *Nature Geoscience*, 5, 601–606.

Tyler, J.J., Jones, M., Arrowsmith, C., Allott, T. & Leng, M.J. (2016) Spatial patterns in the oxygen isotope composition of daily rainfall in the British Isles. *Climate Dynamics*, 47, 1971–1987.

Tyler, J.J., Leng, M.J. & Arrowsmith, C. (2007) Seasonality and the isotope hydrology of Lochnagar, a Scottish mountain lake: implications for palaeoclimate research. *The Holocene*, 17, 717–727.

Verbruggen, F., Heiri, O., Reichart, G.J. & Lotter, A.F. (2010b) Chironomid $\delta^{18}O$ as a proxy for past lake water $\delta^{18}O$: a Lateglacial record from Rotsee (Switzerland). *Quaternary Science Reviews*, 29, 2271–2279.

Waelbroeck, C., Kiefer, T., Dokken, T., Chen, M.-T., Spero, H.J., Jung, S. et al. (2014) Constraints on surface seawater oxygen isotope change between the Last Glacial maximum and the Late Holocene. *Quaternary Science Reviews*, 105, 102–111.

Wassenburg, J.A., Dietrich, S., Fietzke, J., Fohlmeister, J., Jochum, K.P., Scholz, D. et al. (2016) Reorganization of the North Atlantic Oscillation during early Holocene deglaciation. *Nature Geoscience*, 9, 602–605.

Watts, W.A. (1984) The Holocene vegetation of the Burren, western Ireland. In: Haworth, E.Y. & Lund, J.W.D. (eds) *Lake sediments and environmental history*. Leicester: Leicester University Press. pp. 359–376.